Improved Microparticle Electrodynamic Ion Traps for Physics Teaching

Kenneth G. Libbrecht and Eric D. Black
Department of Physics, California Institute of Technology
Pasadena, California 91125

Abstract. We review the essential physics of microparticle electrodynamic ion traps (MEITs) and suggest several improvements in the design, construction, and application of MEITs in undergraduate physics teaching. Pulling together insights gleaned from a number of disparate sources, we have developed MEITs with better overall performance and reliability in comparison to previous publications. This work builds upon a long history of MEIT advancement over many decades, further lowering the barriers to using these fascinating devices in physics teaching labs and demonstrations.

1 Introduction

Electrodynamic ion traps (EITs), also known as Paul traps or quadrupole ion traps, guide the motion of charged particles using time-varying electric fields, thus confining charged particles in free space. Wolfgang Paul and Hans Dehmelt received the Nobel Prize for Physics in 1989 for developing ion trapping, and the technology is in widespread use today. Applications of atomic and molecular ion traps in physics and chemistry include precision mass spectrometry [1], quantum computing [2], and improved atomic frequency standards [3]. In these applications, EITs typically operate using radiofrequency electric fields in vacuum, and they have been well studied over many decades [1, 4, 5]. Microparticle electrodynamic ion traps (MEITs) are also commonly used to measure the detailed properties of individual charged particles in the 100-nm to 100-μm size range, including aerosols [6, 7], liquid droplets [8, 9], solid particles [10, 11, 12], nanoparticles [13, 14], and even microorganisms [15, 16].

MEITs are an excellent addition to physics teaching labs and lecture demonstrations as well, as they provide a fascinating demonstration of oscillatory mechanics and electric forces – both fundamental topics that are taught quite early in undergraduate curricula. Moreover, MEITs are inexpensive to construct, easy to use, and captivating to watch, making them well suited for a teaching environment [10, 17, 18]. Besides individual particles, MEITs can also trap large numbers of charged particles that self-organize into Coulomb crystalline structures [10, 18, 19].

We recently developed a series of MEIT experiments for use in undergraduate teaching labs [20], trapping 26-μm-diameter particles in air using 60 Hz electric fields with electrode voltages up to 6 kV. Load resistors limit all currents to below one mA, making the high-voltage hardware safe for student use. The MEITs themselves are a few centimeters in size, and the particles are illuminated using laser light to make them easily visible to the naked eye.

During our development process, we accumulated a number of valuable insights relating to MEIT design, construction, and operation. Some of these insights are only hinted at in the scientific literature, and others appear only in online videos and other impermanent and hard-to-locate sources (described in detail below). Taken together, these insights greatly improved the performance, reliability, and safety of our MEIT experiments. We now easily trap large numbers of particles in "Coulomb clouds" using a simple ring electrode geometry, and several examples are shown in Figure 1. A principal goal of this paper is to document our experimental methods in detail, as we believe there is much room for additional improvements and creative implementation of MEITs in undergraduate teaching.

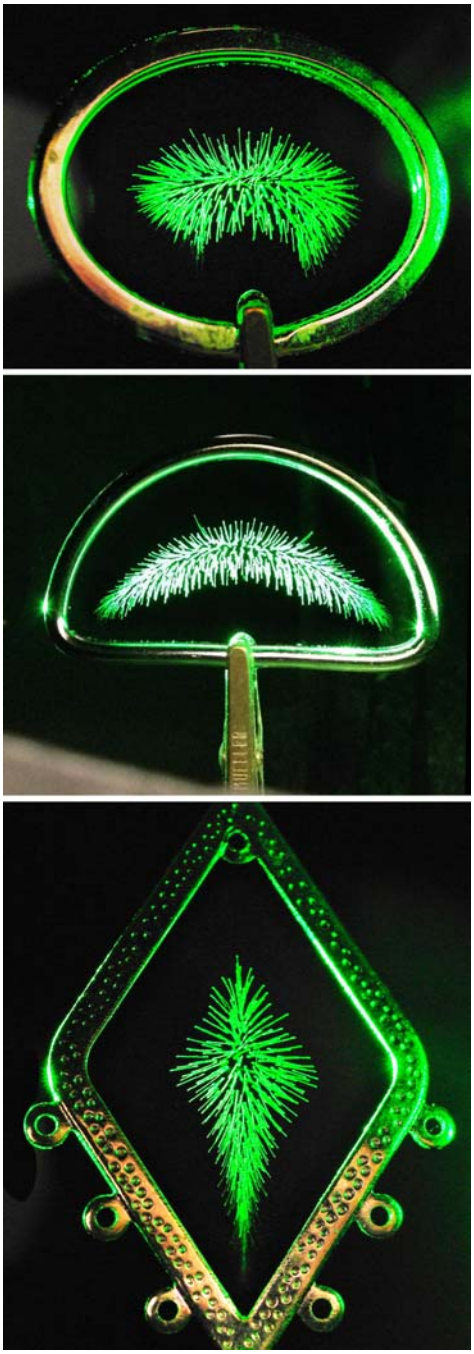

Figure 1. These three photographs show collections of 26-μm-diameter particles trapped in air by ring-type microparticle electrodynamic ion traps (MEITs). Each trap consists of a planar conducting ring electrode held by an alligator clip delivering a voltage of 6 kV AC at 60 Hz. The particles are negatively charged Lycopodium club-moss spores illuminated with laser light. The electric field geometry and trapping forces are described in detail in the text. The particles exhibit oscillatory motions that makes them appear as streaks of light in these photos. The inward trapping forces are countered by the mutual Coulomb repulsion between the particles, resulting in an expanded "Coulomb cloud" with an overall shape defined by the different ring geometries. The oval key ring (top), D buckle (middle) and diamond-shaped earring (bottom) have maximum horizontal inner diameters of 30, 38, and 22 mm, respectively.

2 Basic Ion Trapping Theory

We begin with an introduction to the physics of electrodynamic ion traps, focusing on trapping microparticles in air using 60-Hz electric fields. Many ion-trapping research papers jump quickly to the Mathieu equation to describe the particle dynamics, but that approach (in our opinion) needlessly obscures the underlying physical concepts. Ion trapping requires little more than basic mechanics with Coulomb forces, and thus is quite accessible to beginning physics students and non-physics majors. As we show below, electrodynamic ion trapping can even be described qualitatively using minimal mathematics along with some physical intuition. Since particle levitation and trapping using oscillatory forces is a nontrivial result, electrodynamic ion trapping gives students an intriguing look at what is possible when $F = qE$ is taken beyond simple static situations.

2.1 Earnshaw's Theorem

The basic idea of an ion trap is to confine a charged particle in free space (away from any other matter) using electric fields alone. Samuel Earnshaw showed in 1842 that stable trapping was not possible using static fields, a result now known as *Earnshaw's theorem*. The essential proof is relatively simple (given the benefit of post-1842 physics). To trap a positively charged particle at some position in space, all the electric field vectors around that position would have to be pointing inward. Gauss's Law tells us that this is impossible unless there is a net negative charge at that position. Thus a static electric field geometry cannot stably trap a charged particle in free space.

There are magnetic variations of Earnshaw's theorem as well, stating that a bar magnet cannot be trapped in free space using only static magnetic fields [21]. Adding gravity does not improve matters, and another extension of Earnshaw's theorem states that neither charged particles nor magnets cannot be stably levitated against gravity using static fields alone.

Fortunately, there are many routes around Earnshaw's theorem. One popular engineering method is to use active feedback. In the magnetic case, for example, one can continually measure the position of a levitated magnet and adjust the forces appropriately to keep the magnet stably positioned in free space, which is done in applications ranging from magnetically levitated trains to magnetically levitated toys. Another way around Earnshaw's theorem for magnetic levitation is to use a spinning magnet (possessing non-zero angular momentum) instead of a stationary one. A toy called the *Levitron* demonstrates levitation of a spinning magnet without using active feedback, and magnetic atom traps work using similar principles [22].

Paul and Dehmelt got around Earnshaw's theorem by using oscillating electric fields to trapped charged particles, since the theorem strictly applies only to static fields. Levitating bar magnets using oscillating magnetic fields has also been demonstrated [23]. It is not immediately obvious that you can use oscillating fields to trap particles (hence the Nobel Prize), so our first task as educators is to describe the basic physics underlying electrostatic ion trapping as simply as possible.

2.2 A Mathematics-Free (almost) Description

2.2.1 Particle Motion in a Uniform, Oscillating Electric Field

To begin, consider a charged particle placed inside an ideal parallel-plate capacitor, as shown schematically in Figure 2. Assume that the plates are large compared to their separation, and there is a vacuum between the plates. Assume also that a sinusoidally oscillating voltage is applied across the plates, giving a uniform. oscillating electric field $E(t)$ between the plates, as shown in the Figure.

Between these plates we place a particle having charge q at some position z, with zero initial velocity. The electric force on the particle is given by $F = qE$, and we will ignore the gravitational force. Since the electric field oscillates and thus reverses direction with time, so does the force on the particle, and the particle is pushed up and down as the force on it oscillates. Since the electric field is uniform between the plates, the net force averages to zero over a single cycle. The particle thus oscillates up and down with some fixed average position $\langle z \rangle$. Note that the particle

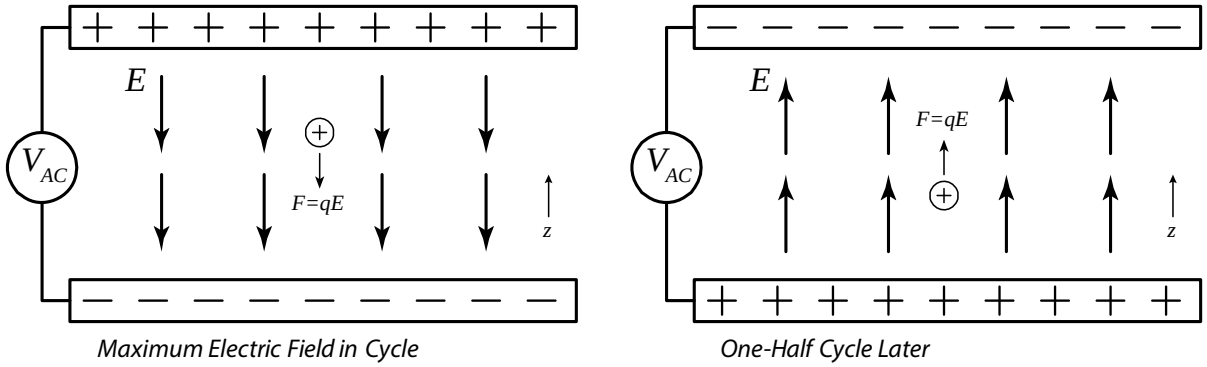

Figure 2. These diagrams shows a charged particle placed initially at rest inside a parallel-plate capacitor. An oscillating voltage is applied to the capacitor, so the electric field oscillates with time, but is always uniform between the plates. The field causes the particle position to oscillate, and two times are shown in these two sketches. Note that when the particle position z is high (left), the electric field pushes it down. When the particle z is low (right), the electric field pushes it back up. The average particle position $\langle z \rangle$ remains constant.

position is 180 degrees out of phase with the applied force, as is shown graphically in Figure 2. When the particle is up (relative to $\langle z \rangle$), the force pushes it back down. And when the particle is down, the force pushes it back up again.

2.2.2 Adding an Electric Field Gradient

Now we make the problem a bit richer by adding a small electric field gradient, so the field is no longer uniform in space. One way to add a field gradient is by curving the plates of our capacitor a small amount, as shown in Figure 3. For example, the two plates in the figure might be sections of spherical shells, where the geometrical centers are both located at the same point high above the plates. The details of the plate geometry are not especially important. What is important is that the electric field lines look roughly like those shown in Figure 3 – in particular, the field strength near the top plate is higher than near the bottom plate (as shown by the lengths of the field vectors in the Figure.)

Since the plates are only curved a small amount, the electric fields differ only slightly from the parallel-plate example shown in Figure 2. The particle motion, therefore, is about the same as it was before, so the particle mainly oscillates about its initial position. But now we can see, from the geometry in Figure 3, that the force over one cycle no longer averages to zero. As shown in the Figure, when z is above $\langle z \rangle$ (left side of the figure), the particle experiences a stronger-than-average electric field pushing it downward. And when z is below $\langle z \rangle$ (right side of the figure), the upward force is weaker than average. This imbalance was not present in Figure 2. From this fairly basic reasoning, shown graphically in Figure 3, we can deduce that there is a net force pushing the particle down. Put another way, the force averaged over many oscillation cycles pushes the particle toward a region where the oscillating electric field is weaker.

2.2.3 Quadrupole Ion Traps

With this basic understanding of how particles behave in oscillating electric fields, we can proceed to make an ion trap by considering more complex field geometries. We will focus on what are called *quadrupole ion traps*, looking at both 3D and 2D varieties. One easy way to make a 3D quadrupole trap is shown in Figure 4. An AC voltage is applied to two ball-shaped electrodes in a grounded box, creating oscillatory electric fields inside the box. Halfway between the balls, the electric field is always zero by symmetry. Near this zero-field point, the electric fields at one point in the AC cycle are shown in the Figure. Multiply these vectors by $\sin(\omega t)$ to obtain the electric fields at other times.

With this field geometry, the electric field strength increases in all directions outward from the zero-field point

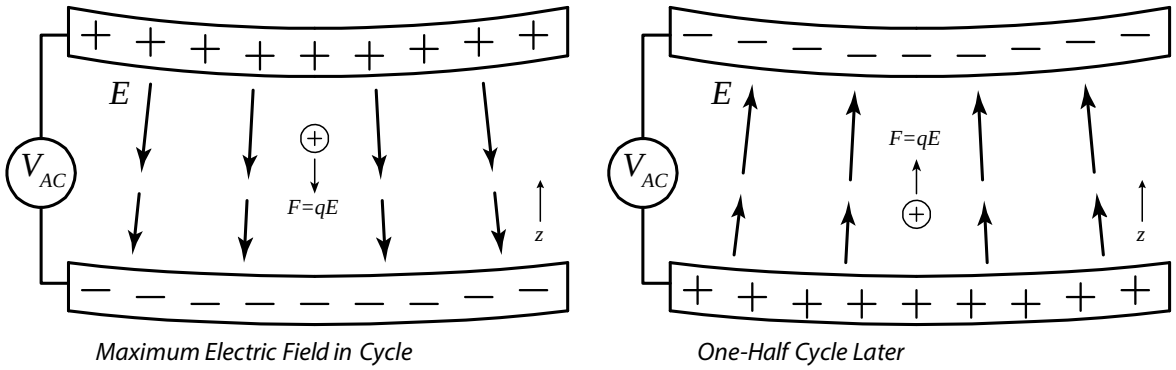

Figure 3. A charged particle placed initially at rest inside a curved-plate capacitor. The geometry of the plates causes a gradient in the electric field strength, so that the field is stronger for larger z (as shown by the longer arrows in the diagrams) This imbalance means that the electric force on the particle is stronger at the top of its motion (left) and weaker at the bottom (right). Averaging over time, there is a net force that pushes the particle down, toward the weaker-field region.

halfway between the balls. Since the time-averaged electric forces push particles toward regions where the oscillating electric field is weaker, particles become trapped at the center point.

The qualitative force argument shown graphically in Figure 3 strictly only applies to the $r = 0$ line and the $z = 0$ plane in the ball-trap (taking $r = z = 0$ at the center point between the balls). One can, however, draw pictures similar to those in Figure 3 that examine a particle placed at other locations in the trap, for example when $r = z \neq 0$. Doing this quickly reveals that the time-average of the (vector) electric force again pushes the particle toward the trap center at $r = z = 0$.

It is customary to divide the particle motion into two parts: 1) the *micromotion* that occurs on 60-Hz time scales, and 2) the *secular motion* that is averaged over several oscillation periods. For the quadrupole trap shown in Figure 4, the micromotion is zero at the trap center and increases in all directions away from this point. The secular motion arises from the time-averaged forces that push particles toward the trap center.

Another approach for making a 3D quadrupole trap is the *ring trap* shown in Figure 5. Again the electric field at the center of the ring is always zero, and the arrows show the fields in the vicinity of this central region at one point in the cycle. Both these examples show electric field geometries that: 1) have zero electric field at a center point, 2) have field magnitudes that increase in all directions away from the central point, and 3) exhibit axial symmetry.

With the above qualitative description, it is possible to explain ion trapping while standing at the chalkboard, using vector diagrams and essentially no equations. All that is required is a basic understanding of mechanics and electric forces. The most difficult concept is the quadrupole field geometry. Interestingly, our intuitive feel for electric-field geometries appears to have come entirely (or almost entirely) from seeing vector field diagrams in physics classes, in physics demonstrations, and in textbooks. The actual calculation of these vector plots is nontrivial and is learned much later in physics curricula. A discussion of electrodynamic ion trapping, therefore, helps to establish and reinforce this learned intuition.

2.3 A Basic Mathematical Description

To quantify the above qualitative description, assume that the plates in Figure 2 are separated by a distance d, and the applied voltage is $V(t)$. As long as the fields do not change too rapidly, we can assume a uniform electric field in the space between the plates equal to $E(t) = V(t)/d$. Assume a sinusoidally oscillating voltage, $V(t) = V_0 \sin \omega t$, which gives an electric field between the plates $E(t) = E_0 \sin \omega t$, with $E_0 = V_0/d$. The time-dependent electric

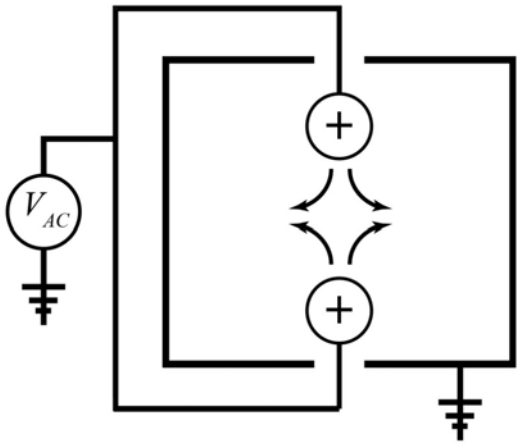

Figure 4. This diagram shows one method for making a 3D quadrupole ion trap, using two ball-shaped electrodes in a grounded box. When the balls are at a positive potential relative to the box, as shown here, the electric field lines are given roughly by the arrows. A half-cycle later, the balls are at a negative potential relative to the box, and the field lines are reversed. By symmetry, the electric field halfway between the balls is always zero. The electric field geometry between the balls is essentially as drawn here even if the grounded walls of the box are expanded out to infinity.

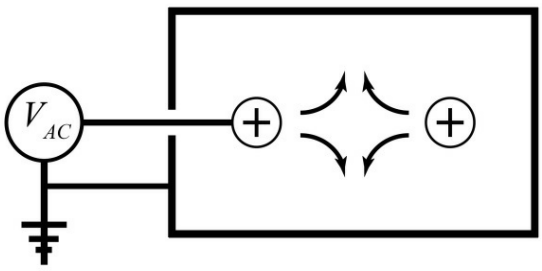

Figure 5. This diagram shows another method for making a 3D quadrupole trap. In this configuration a ring electrode (seen edge-on here) is placed inside a grounded box, and the potential between the two is set by an applied AC voltage. As in Figure 4, the electric field at the ring center is always zero by symmetry. Also, the electric field geometry near the ring center is essentially as drawn here even if the grounded walls of the box are expanded out to infinity.

force on the particle is $F(t) = qE(t) = qE_0 \sin \omega t$, and solving this equation of motion gives the particle position

$$z(t) = z_{init} + v_{init}t - \frac{qE_0}{m\omega^2} \sin \omega t \tag{1}$$

where z_{init} is the initial position of the particle and v_{init} is its initial velocity. This quantifies the result shown graphically in Figure 2, showing that the particle micromotion is 180 degrees out of phase with the applied force.

Adding a field gradient and taking $z_{init} = v_{init} = 0$, the force on the particle becomes

$$F(z,t) = q\left(E_0 + E'z\right) \sin \omega t \tag{2}$$

where $E' = dE/dz$. For small E', we substitute the micromotion in Equation 1 as an approximation for $z(t)$ in Equation 2, giving the approximate time-averaged (secular) force

$$\langle F \rangle \approx -\frac{q^2 E' E_0}{2m\omega^2} \tag{3}$$

We leave it as an exercise for the reader (using perturbation theory) to show that this result is rigorously accurate to lowest order in E'. The negative sign in this expression means that $\langle F \rangle$ pushes the particle toward a region of weaker electric fields. Note also that the trapping force is independent of the sign of the charge.

A convenient way to think about this is with a trap *pseudopotential* that is simply the kinetic energy of the micromotion: $U_{trap} = (KE)_{micromotion} = \frac{1}{2}mv^2_{micromotion}$. The secular force in the vertical direction is then equal to the gradient $\langle F \rangle = dU_{trap}/dz$, giving Equation 3 in the example above. It turns out that $\langle F \rangle$ is equal to the gradient of the pseudopotential in all three dimensions (for example in a quadrupole electric field geometry), but proving this is beyond the scope of this paper. A general derivation of the pseudopotential $U_{trap} = (KE)_{micromotion}$, along with a careful consideration of the underlying assumptions, is given in [24] (Section 30).

2.4 Quadrupole Field Geometries

We can quantify the quadrupole electric field geometries by looking at the fields near the trap center. A multipole expansion of a 3D quadrupole trap gives an electric potential near $r = z = 0$

$$V(r,z)_{3D-Quad} = A_0 + A_2\left[2z^2 - r^2\right] \cos \omega t$$

where A_0 and A_2 are constants, with the electric fields

$$\begin{aligned} E_z &= -\frac{\partial V}{\partial z} = -4A_2 z \cos \omega t \\ E_r &= -\frac{\partial V}{\partial r} = 2A_2 r \cos \omega t \end{aligned} \tag{4}$$

and a vector plot is shown in Figure 6. Note that the electric field strength increases linearly with r and z as one goes out from the origin.

For a 2D quadrupole trap, we have

$$V(x,y)_{2D-Quad} = A_0 + A_2\left[x^2 - y^2\right] \cos \omega t$$

giving the electric fields

$$\begin{aligned} E_x &= -\frac{\partial V}{\partial x} = -2A_2 x \cos \omega t \\ E_y &= -\frac{\partial V}{\partial y} = 2A_2 y \cos \omega t \end{aligned} \tag{5}$$

Rotating the potential by 45 degrees in the xy plane gives a similar-looking expression

$$\begin{aligned} E_x &= -2A_2 y \cos \omega t \\ E_y &= -2A_2 x \cos \omega t \end{aligned} \tag{6}$$

and a vector plot is shown in Figure 7. Again we see that the electric field strength increases linearly with x and y near the origin.

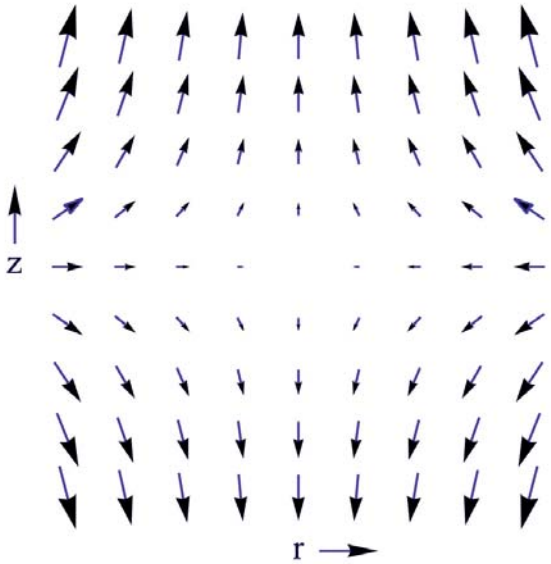

Figure 6. A vector plot of the 3D quadrupolar electric field geometry, showing the electric field vectors when the applied voltage is at its maximum. Multiply each vector by $\cos(\omega t)$ to obtain the electric fields at other times. Note that the field amplitude in the z direction (along $r = 0$) is double that in the r direction (for $z = 0$). Both the ring trap and the single-particle trap described in the text have this field geometry near the trap center.

2.5 Damped Ion Traps

Damping is important for our MEITs operating in air, so we add a viscous damping force $F = -\gamma v$, where γ is the usual damping constant and v is the particle velocity. The one-dimensional case can be computed in much the same way as we described above, giving the secular force

$$\langle F \rangle \approx -\frac{q^2 E' E_0}{2m} \frac{1}{\omega^2 + \Gamma^2} \tag{7}$$

where $\Gamma = \gamma/m$, and this reduces to Equation 3 in the absence of damping. The same result can also be obtained using the pseudopotential U_{trap} described above.

2.5.1 Stokes Damping

To calculate the damping constant, we first note that the Reynolds number of the particle motion is quite small, given by $R_e \approx \rho_{air} v R/\mu_{air} \approx 0.05$, where $\rho_{air} \approx 1.2$ kg/m^3 is the air density, $v \approx 1$ mm/(1/60 sec) ≈ 6 cm/sec is a typical observed particle micromotion velocity in a trap, $R \approx 13$ μm is the particle radius (described below), and $\mu_{air} \approx 1.8 \times 10^{-5}$ kg/m-s is the dynamical viscosity of air. For such a low Reynolds number, the air damping is well approximated by Stokes damping, given by $\gamma = 6\pi\mu R$. Assuming a particle density of $\rho_{part} \approx 500$ kg/m^3, this gives

$$\Gamma = \frac{\gamma}{m} = \frac{9}{2} \frac{\mu}{R^2 \rho_{part}} \approx 960 \text{ s}^{-1}$$

which is substantially larger than $\omega = 2\pi(60 \text{ Hz}) = 377$ s^{-1}. Thus the particle motion is overdamped and $\omega^2 + \Gamma^2$ in Equation 7 can be replaced with Γ^2 to an accuracy of about 15 percent.

2.5.2 Trap Stability

The above calculations of secular forces are useful for estimating trap forces and showing the basic trap physics. In many applications of ion trapping (e.g., molecular mass spectroscopy), another important consideration is the

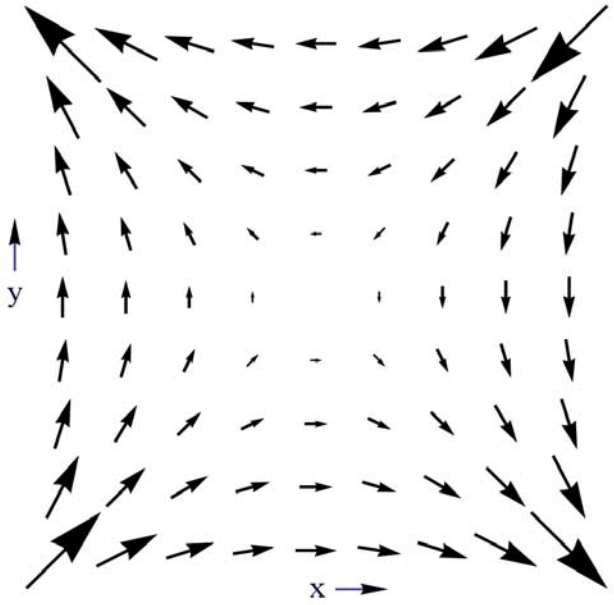

Figure 7. The 2D quadrupolar electric field geometry, again plotting the electric field vectors at one point in time. The "4-bar" linear trap described in the text has this field geometry near its central axis.

stability of trapped ions. In the zero damping case, stably trapped particles in an ion trap will execute complex bound orbital motions that depend on initial conditions [25, 5]. As the applied trapping voltage is turned up, eventually the oscillating electric fields eject particles from the trap and stable trapping is no longer possible. Analyzing ion trap dynamics to determine stability is where the Mathieu equation formalism becomes necessary.

When linear damping is added, such as Stokes damping, a trapped ion will either come to rest at the trap center (ignoring gravity or other static forces), or be ejected from the trap, as determined by the Mathieu-equation analysis [26]. Interestingly, the MEITs described below include a rich behavior of what we call "extended orbits", which require the addition of a weak nonlinear damping term in addition to Stokes damping [27].

Obtaining a full understanding of ion trap dynamics, including nonlinear dynamics, is still an area of active research, and it lies beyond what is typically presented in undergraduate curricula. However, the basic trap analysis described above shows that the essential EIT physics is mainly mechanics and electric forces, topics that are taught in early college physics courses. For this reason, ion traps provide a useful tool for connecting basic physics concepts to a nontrivial and quite fascinating application. A mention of trap stability, mass spectroscopy, and nonlinear dynamics has pedagogical merits as well, in that it informs students that physics remains a dynamic subject where relatively simple concepts factor into many modern applications. Our attention now turns to methods and practices that are useful when constructing MEITs for applications in physics teaching.

3 MEIT Design and Construction

As mentioned in the introduction, the use of MEITs in physics education has been presented in the literature numerous times [17, 18, 19, 10]. With these papers as a starting point, we begin by describing several insights we have gained during the design and construction of our own ion trapping experiments.

3.1 Laser Illumination

Individual particles in the 10-30 μm size range are very difficult to see with the naked eye when illuminated by

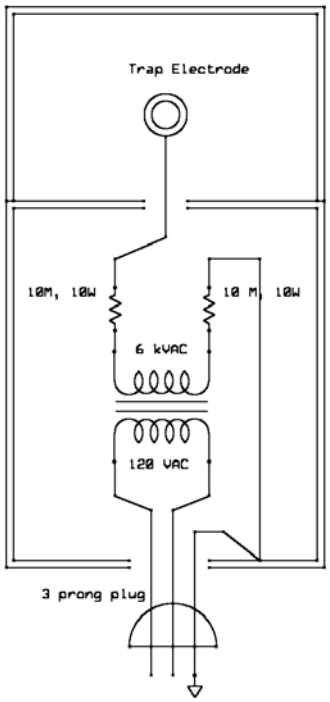

Figure 8. This diagram shows a schematic of a basic single-electrode ion trap, with redundant current-limiting, as described in the text.

ambient room lights, and trapped particles can be overlooked even with bright, directed incandescent or LED lighting. Laser illumination, however, changes this dramatically, making the particles easily visible [28]. We typically use inexpensive 10 mW green laser modules (which often put out 20 mW or more of 532 nm light), and we expand the beam to roughly a 1-cm size. A 1-cm beam is sufficient to illuminate all the particles in a typical ion trap, and the eye-safety concerns from such an expanded beam are no worse than with a typical green laser pointer. Laser illumination was not mentioned in many previous discussions of MEITs, and it makes a huge difference when observing trapped particles.

3.2 The 6 kV Solution

In general, we have found that higher applied AC voltages yield more robust MEITs that are easier to use and can hold a larger numbers of particles. The improvement appears to come from trap loading considerations, although we have not explored all regions of parameter space in trap design. We believe that higher voltages mean that larger trap electrodes can be used, with an accompanying increase in the effective capture volume during loading. In our experience, trapping with 1 kV is possible but not trivial with typical trap designs and particle charging (see below), and clear improvements are seen as the voltage is increased. Around 10 kV, however, the trap electrodes can readily arc without careful electrode design. We have found that 6 kV of applied AC voltage is a reasonable compromise, yielding excellent trap performance with minimal arcing. Suitable commercial transformers that can produce such high voltages are both expensive and difficult to find, however, so we had our 6kV transformers built to order.

3.3 Current Limiting

Although MEITs operate at high voltage, they require very little current. Thus MEITs present little electrical safety hazard as long as sufficient current-limiting is provided. We typically use load resistors to keep currents to below 1 mA in our MEIT designs, as this is near the limit of human detectability. Moreover, our electrodes have quite low

capacitance, so the stored electrical energy is less than can be experienced from static shocks in carpeted rooms.

Figure 8 shows a relatively simple "one-electrode" trap circuit and electrode geometry, which was used to create the ion trap photos shown in Figure 1. A pair of 10 MΩ, 10W resistors limit the current at the output of the step-up transformer to less than 1 mA. The two resistors provide redundant safety; if one resistor shorts, the other still limits the output current. Additional safety is provided by carefully mounting the transformer and current-limiting resistors in a rugged, sealed metal enclosure that is grounded to the third prong of the AC plug. Thus if any circuit element shorts to the case, the resulting current is shunted to ground. Quite a lot would have to fail in this circuit before the trap user experienced a dangerous electrical shock. Even touching the trap electrode directly would only give a mild shock.

3.4 Triboelectric Particle Charging

The triboelectric effect provides a convenient and inexpensive method to charge particles before insertion into a MEIT. We charge the tip of a teflon "wand" by rubbing it with cloth, and then use the wand to pick up and deliver charged particles to the trap. Holding the wand tip above the trap while tapping it to release particles is most effective. Used in this way, a Teflon wand yields negatively charged particles, while a Nylon wand gives positively charged particles, as expected from the triboelectric series. We have found that Teflon is more effective than Nylon as a wand material, in that it typically delivers more particles to the traps with greater ease. This triboelectric effect provides a simple method for charging nonconducting dielectric particles that is substantially more effective than the syringe method described in [17].

3.5 Lycopodium Club Moss Spores

Lycopodium club moss spores are nearly ideal for trapping in MEITs, since they are inexpensive, readily available, a convenient size, nearly monodisperse, nearly spherical, easily charged, and they present essentially no safety concerns. Their use in this regard is mentioned in the comments section at [30], but we have not seen any other mention in the scientific literature. We purchased our spores online, where they are often called *Dragon's Breath*, as the particles are used to "breathe fire" in magic shows and similar events. As shown in Figure 9, the particles have a characteristic "sphere with a corner" shape. Approximating the particles as spheres, we measured particle diameters of 26 ± 2.5 μm and a material density of 510 ± 40 kg/m^3. However, we have not done an exhaustive comparison of particle properties from different batches or different vendors. There are hundreds of known species of club moss, many quite common in temperate climates, and, to our knowledge, breathing or ingesting club moss spores in small quantities presents essentially no safety concerns.

3.6 Reduce Air Currents

The trapping forces in a MEIT are sufficiently small that air currents can easily blow particles out of a trap. This can make it difficult to trap particles in open areas like teaching labs or lecture halls without mitigating this problem. We typically surround our MEITs with enclosures that have small holes for inserting and observing particles. For the best trap stability, we block these holes completely when not in use, or cover them with optical windows.

3.7 Avoid Triboelectric Materials in MEIT Construction

Surface charging can produce sizeable spurious electric fields if plastics or other triboelectric materials are placed near the trapping region. We typically use metal construction where possible, and keep plastics away from the trapping region as much as possible. Wood and cardboard are useful materials for shielding air currents, as these materials do not develop surface charges as readily as most plastics.

3.8 Strobe the Illumination Laser

Trapped particles in a MEIT typically display a substantial micromotion, making the particles appear as short streaks

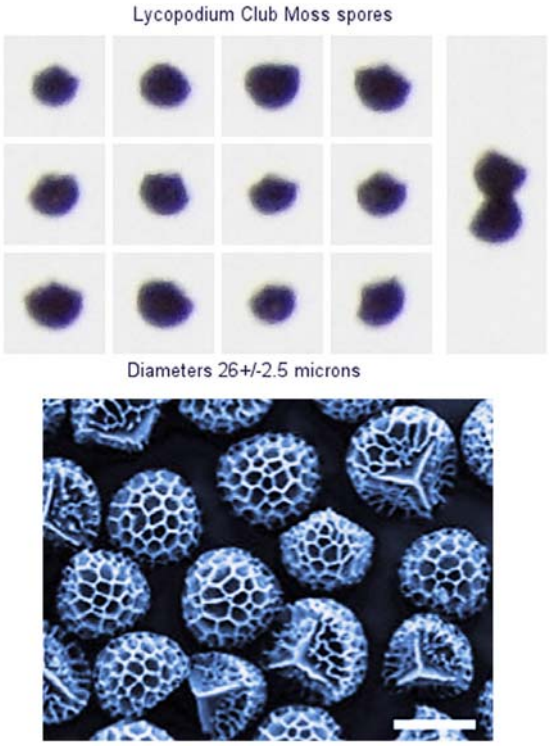

Figure 9. The top images show a series of Lycopodium club moss spores photographed while they were trapped in a MEIT. Each of the 12 images is 57 μm square, and the particles were measured to have diameters of 26 ± 2.5 μm. These 12 particles were trapped consecutively and were not otherwise selected. The additional image on the right shows two spores stuck together while trapped, as is occasionally seen. The lower image is a high-resolution electron micrograph of Lycopodium spores [29], with a scale bar of 25 μm. Note that the characteristic "sphere with a corner" shape can be seen in the optical images, which have a resolution of about three microns. We measured the average material density in the spores, giving $\rho = 510 \pm 40$ kg/m^3.

of light, and these are often misinterpreted by novice observers. Strobing the illumination laser near the trapping frequency demonstrates the micromotion and is quite useful as a pedagogical tool when students first see an ion trap. Video examples can be seen at [20].

3.9 Use Static Fields to Balance Gravity

Gravitational forces are sufficient to pull trapped particles substantially away from the trap center, and this effect is readily seen when a single particle is trapped. Gravity is easily balanced, however, by adding a static electric field with $qE = mg$. Modular DC-DC converters are especially useful for providing the necessary high voltages, since essentially no current is needed.

3.10 The Single-Electrode Trap

It is often beneficial to use a single trap electrode in a MEIT, letting the effective ground far from the trap serve as the second electrode. Examples are the ring traps shown in Figures 1 and 8, or the linear "paper-clip" trap shown in [30]. These trap geometries are especially open, allowing clearer views of the trapped particles than traditional trap geometries with multiple electrodes [17]. Moreover, one can be remarkably cavalier with the second electrode; it is not necessary to have a conducting grounded surface near the trapping region.

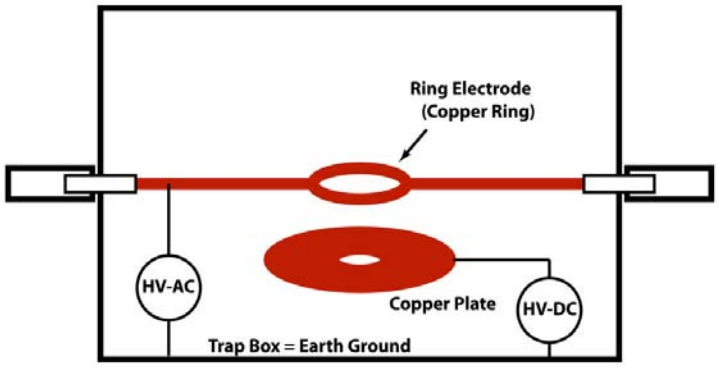

Figure 10. This diagram shows our typical *ring trap* geometry. The main trap electrode is a copper ring (16 mm inner diameter) that can be rotated about a horizontal axis, and this is surounded by a grounded metal enclosure. Ions are trapped near the center of the ring, as shown in Figure 11. A conducting plate below the ring provides a static electric force to approximately balance the gravitational force.

4 The Ring Trap

The construction insights described in the previous section are all demonstrated in the *ring trap* shown schematically in Figure 10. The AC electrical circuit is that from Figure 8, which provides ample current-limit protection. A single copper ring with an inner diameter of 16 mm serves as the main trap electrode, and the ring can be rotated about a horizontal axis (by twirling the insulated handles outside the box) to provide different views the trapped particle cloud. The lower DC electrode shown in Figure 10 provides a static electric field to roughly balance gravity. The ring electrode is surrounded by a metal enclosure that serves as an electrical ground, and the enclosure also greatly reduces air currents. An illumination laser shines down through the ring from above (not shown in Figure 10). A large hole in the front of the box is used to see the trap directly with the naked eye and to insert the wand for loading, and this hole is typically blocked once particles are loaded (to further reduce air currents). Trap imaging is done through a window in the back of the box.

Figure 11 shows a small collection of particles in a ring trap, and Figure 12 shows a much larger number of particles trapped. In our physics teaching lab, we use the ring trap as a qualitative demonstration of ion trapping physics. Students are introduced to the basic trapping theory presented above, including secular and micromotion forces, quadrupolar electric field geometries, the triboelectric effect, Coulomb crystals, and laser strobing. Students load particles into the trap (both positively and negatively charged using Nylon and Teflon wands), and view the trapped particles with the naked eye and via video imaging. The AC and DC trapping fields can be varied in amplitude to examine the trap response. The DC electric fields are used to identify positively and negatively charged particles. The DC field can also balance gravity to trap a single particle with essentially no remaining micromotion at the center of the ring. The micromotion of the particles traces out the quadrupole electric field geometry, as demonstrated in Figure 12.

5 The Linear Trap

Figure 13 shows a schematic layout of a *linear trap*, which traps particles along a line using a 2D quadrupolar electric field geometry. Teflon end caps develop a negative surface charge as the trap is used (presumably as negatively charged particles impinge upon the inner surface of the tubes), and this charge is sufficient to weakly trap negatively charged particles in the axial direction. Here again we exploit the triboelectric effect as an inexpensive method for providing the desired axial electric fields. For both the linear and ring traps, students can literally poke at

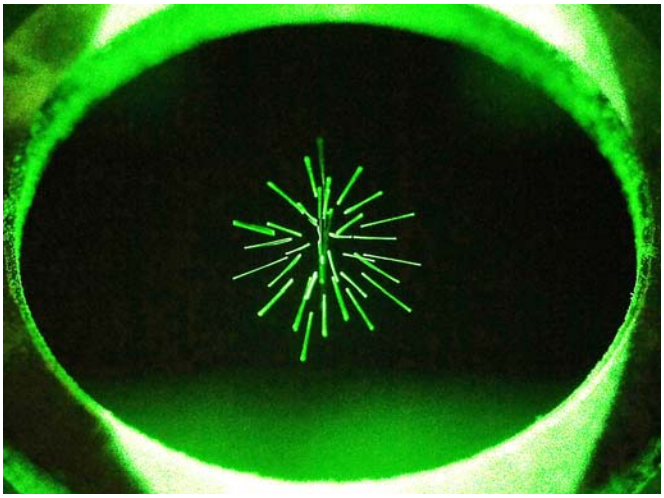

Figure 11. This photograph shows about 30 particles held in a ring trap, which is illuminated from the top with laser light. Trapping forces push particles toward the center of the ring, while their mutual Coulomb repulsion keeps them apart. The 60-Hz micromotion makes each of the particles appear as a streak of light in this photograph, which is how they appear to the naked eye.

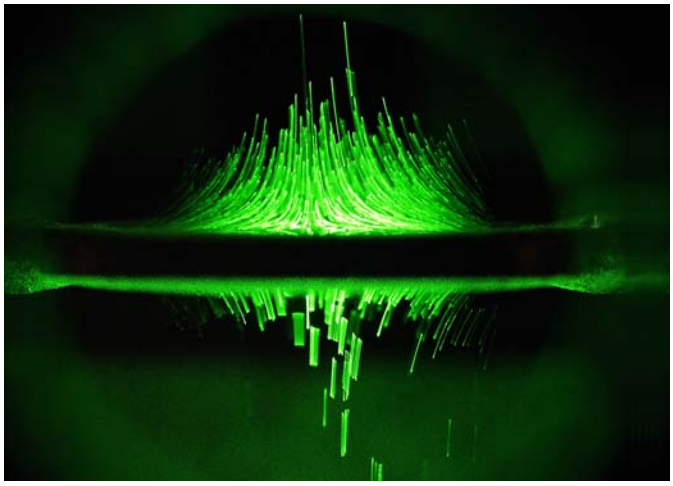

Figure 12. This photograph shows many hundreds of particles held in a ring trap, here with the ring plane nearly horizontal. The micromotion of each particle is along the electric field, so the line segments in the photograph trace the quadrupole electric field geometry within the trap. Static electric fields can push the trapped particles above or below the ring plane.

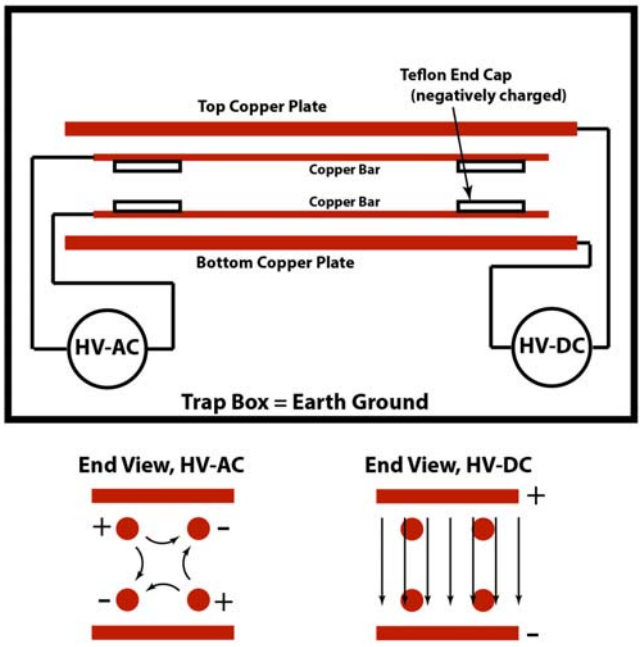

Figure 13. These diagrams show a "4-bar" linear ion trap. The AC and DC electric fields are shown qualitatively in the lower diagrams, which show views along the horizontal trap axis. The top diagram shows a face-on view of the trap. The four trap bars have diameters of 3.2 mm, with a closest separation of 9.5 mm.

the trapped particles with the charged wand to see how this affects the trapping.

Figure 14 shows a linear trap being used to create a one-dimensional Coulomb crystal, after selecting particles with similar charges. In our physics teaching lab, we use the linear trap as another qualitative demonstration of ion trapping physics. Students are introduced to the linear trapping geometry and one-dimensional Coulomb crystals. Additional nonlinear effects are also demonstrated in the linear trap, and these effects are described in detail in [27]. The "trapnado" [27, 20], which can be created easily in the linear trap, provides an especially dramatic example of how many-body effects can lead to nontrivial emergent phenomena, and it reminds students that future physicists have much to ponder even in relatively simple physical systems.

6 The Single-Particle Trap

To go beyond qualitative ion trapping phenomena and into quantitative measurements in the teaching lab, we use the *single-particle trap* shown schematically in Figure 15. This trap incorporates a built-in microscope objective (not shown in the figure) that is capable of imaging trapped particles with a resolution of about three microns. Sample images from the microscope are shown in Figure 9, using LED backlighting. With this trap geometry, the DC electric field is linearly proportional to the applied voltage HV-DC with a known proportionality constant. The constant A_2 in Equation 4 is similarly calculated from numerical modeling of the electrode geometry.

The micromotion of a single trapped particle is eliminated when the static electric force balances gravity, and this can be readily observed in the microscope video image. The force balance $qE = mg$ then gives the charge-to-mass ratio q/m for a known applied field E. Imaging the particle gives its radius to about 20 percent, allowing students to calculate the particle mass m from the known material density. Putting the different observations together thus yields the charge q to an overall accuracy of about a factor of two. Typical measurements yield particle charges equal to about 10^5 times the electron charge.

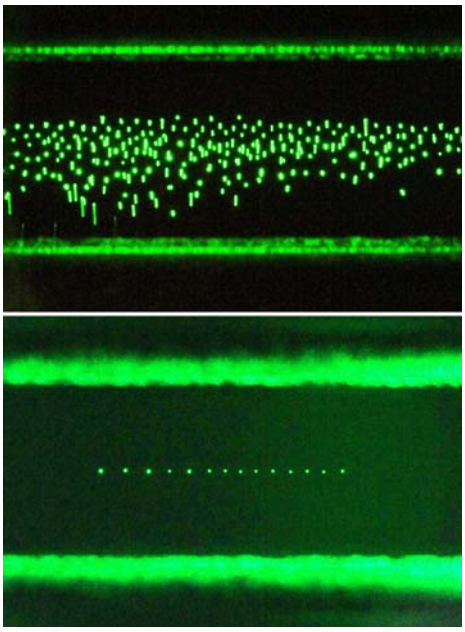

Figure 14. The top photograph shows a large number of particles held in a linear trap, illuminated with laser light. Trapping forces push particles toward the horizontal trapping axis, while their mutual repulsion keeps them separated. The diffuse horizontal lines above and below the trapped particles are from the bar electrodes. The lower image shows 14 particles in a linear Coulomb crystal. Trapping forces keep the particles along the trap axis, and gravity is balanced by static electric forces. The particles are pushed together by weak axial electric fields, and they are held apart by mutual Coulomb repulsion.

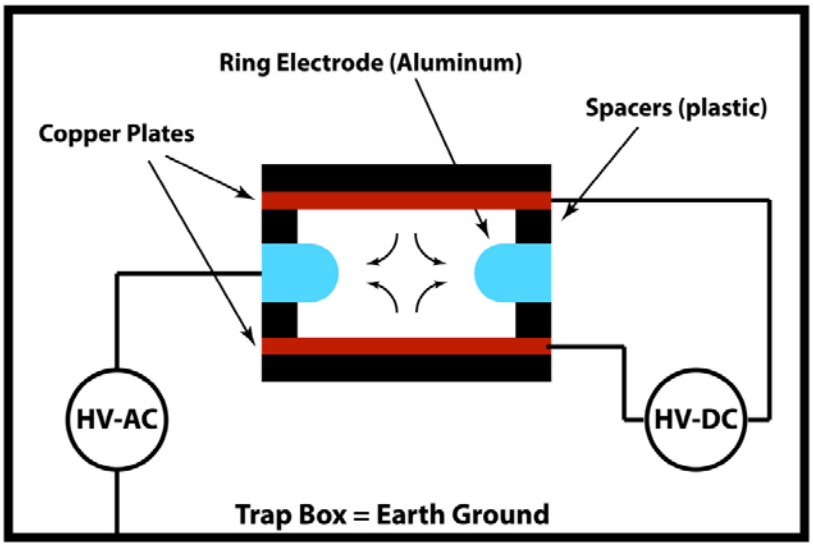

Figure 15. A schematic diagram of the single-particle trap described in the text. The ring electrode is an aluminum plate with a 9.5-mm-diameter central hole, and this is flanked by parallel copper plates (seen edge-on in this diagram; separated by 12.7 mm). Numerical modeling of the axially symmetric electrode geometry relates the electric fields to the applied voltages.

7 Discussion

Having incorporated the various design insights described above, we found that our MEITs were remarkably robust and easy to use. Add to that their simplicity, relatively low cost, intriguing physics content, and overall student appeal, and we believe that ion trapping has a great deal of unrealized potential as a physics teaching tool. Moreover, we believe that ion trapping is brimming with possibilities for intriguing student-led projects with varying levels of difficulty. A few examples include:

1) Measuring light pressure effects. The gravitational force on a Lycopodium spore is approximately 50 pN, equal to the light force from absorbing a 15 mW laser beam. Moreover, gravity is a large and easily observed force in the MEITs described above. With some care, it should be possible to detect forces down to 100 fN or lower in a specially designed MEIT. Thus one should be able to observe light pressure effects using nothing more than a common laser pointer. While this would not be an especially easy or inexpensive experiment, it may end up being cheaper, safer, and more quantitative than the optical-tweezer experiments that have become somewhat popular in physics teaching.

2) Measuring the fundamental charge. A single electron charge in a static field of 10^6 V/m (3x below a typical breakdown field) experiences a force of $qE = 160$ fN. With additional improvements in trap design, we can imagine a MEIT-based experiment capable of measuring the fundamental charge more reliably than the venerable (but difficult) Millikan oil-drop experiment. Observing discrete charge jumps (for example from cosmic rays) on a single MEIT particle would confirm the discrete nature of charge without having to make a precise charge measurement.

3) Exploring different particle materials. Trapping Lycopodium club moss spores in MEITs is a substantial design advance, in our opinion, as these particles allow easier trap operation compared to other choices. However, searching for still better pollen-like particles could be a worthwhile research effort. Exploring methods for obtaining higher particle charges could also be quite fruitful, as higher charges would require lower trap voltages.

4) Examining *in situ* charging and discharging. An individual particle in a MEIT is easily stable for days or weeks [17], but it may be interesting to explore charging or discharging mechanisms, perhaps as a function of particle micromotion, UV illumination, humidity, and other factors. Cold-cathode emission from a thin, sharpened wire placed near a trapped particle may have interesting effects as well. Here again, discovering ways to control the charge on trapped particles could be highly beneficial for developing the next generation of educational MEITs.

5) Investigations of nonlinear dynamics in MEITs. We scratched the surface of this topic in [27] (also see the references therein), but a great deal remains unexplored. Numerically integrating the equations of motion in a MEIT is straightforward using modern computational tools, allowing investigations of trap behavior that do not require complex analytical nonlinear mathematics.

6) Investigating novel trap geometries. As seen in Figure 1, even the basic ring trap can yield a variety of Coulomb cloud shapes. Creating "race track" or other trapping topologies may yield novel trap behaviors, especially in the presence of Coulomb forces between trapped particles and perhaps nonlinear trap effects.

7) Dynamical measurements of particle properties. In the presence of damping, the trapping forces depend on particle radius via Equation 7, and thus it should be possible to determine particle properties using dynamical measurements like micromotion. Nonlinear effects may be important also [27]. Once again, there remains significant potential for finding effects that are important for developing the next generation of MEITs.

8) Mie scattering of spherical particles. An isolated, stationary, 25-micron-scale particle makes an excellent target for laser Mie scattering, which can be used as an independent method of determining the particle radius.

9) Mega MEITs. While we stopped at 6 kV, proper electrode design would allow higher applied voltages, and thus still larger traps that confine more particles. Realizing particles with greater average charges would also be helpful in this regard. Establishing and documenting a record number of trapped particles could lead to some measure of YouTube renown, perhaps generating a bit of student enthusiasm in the process.

As a physics toy and instructional tool, we believe that MEITs provide a great deal of unrealized potential. Many interesting experimental and theoretical avenues have not yet been explored, and there appears to be much opportunity for involving eager physics students in developing the next generation of educational MEITs.

A number of Caltech undergraduate students contributed to the initial development of our ion traps, including Christopher Dewan, John Schulman, Giulio Rottaro, Nathaniel Indik, Gautam Upadhya, Scott Yantek, Prastuti Singh, Max Horton, and Kelly Swanson. This work was supported in part by the California Institute of Technology and by generous donations from Drs. Richard Karp and Vineer Bhansali.

8 References

[1] R. E. March and J. F. Todd, "Quadrupole ion trap mass spectroscopy, 2nd edition" Wiley-Interscience (2005).

[2] H. Haffner, C. F. Roos, and R. Blatt, "Quantum computing with trapped ions," Phys. Rep. 469, 155-203 (2008).

[3] D. Leibfried, R. Blatt, C. Monroe, and D. Wineland, "Quantum dynamics of single trapped ions," Rev. Mod. Phys. 75, 281-324 (2003).

[4] P. K. Ghosh, "Ion Traps," Oxford Univ. Press (1996).

[5] R. E. March, "An introduction to quadrupole ion trap mass spectrometry," J. Mass Spectrom. 32, 351-369 (1997).

[6] M. Yang et al., "Real-time chemical analysis of aerosol particles using an ion trap mass spectrometer," Rapid Comm. Mass Spect. 10, 347-51 (1996).

[7] D. T. Suess and K. A. Prather, "Mass spectrometry of aerosols," Chem. Rev. 99, 3007-3036 (1999).

[8] B. Kramer, O. Hubner, H. Vortisch, et al., "Homogeneous nucleation rates of supercooled water measured in single levitated microdroplets," J. Chem. Phys. 111, 6521-6527 (1999).

[9] S. Arnold and L. M. Folan, "Fluorescence spectrometer for a single electrodynamically levitated microparticle," Rev. Sci. Instrum. 57, 2250–2253 (1986).

[10] R. F. Wuerker, H. Shelton, and R. V. Langmuir, "Electrodynamic containment of charged particles," J. Appl. Phys. 30, 342–349 (1959).

[11] Gina Visan, Ovidiu S. Stoican, "An experimental setup for the study of the particles stored in an electrodynamic linear trap," Rom. J. Phys. 58, 171-180 (2013).

[12] S. Schlemmer, J. Illemann, S. Wellert, et al., "Nondestructive high-resolution and absolute mass determination of single charged particles in a three-dimensional quadrupole trap," J. Appl. Phys. 90, 5410-5418 (2001).

[13] Y. Cai, W.-P. Peng, S.-J. Kuo et al., "Single-Particle Mass Spectrometry of Polystyrene Microspheres and Diamond Nanocrystals," Anal. Chem. 74, 232-238 (2002).

[14] Sung Cheol Seo, Seung Kyun Hong, and Doo Wan Boo, "Single Nanoparticle Ion Trap (SNIT): A Novel Tool for Studying in-situ Dynamics of Single Nanoparticles," Bull. Korean Chem. Soc. 24, 552-554 (2003).

[15] W. P. Peng, Y. C. Yang , M. W. Kang, et al., "Measuring masses of single bacterial whole cells with a quadrupole ion trap," J. Am. Chem. Soc. 126, 11766–11767 (2004).

[16] Zhiqiang Zhu, Caiqiao Xiong, Gaoping Xu, et al., "Characterization of bioparticles using a miniature cylindrical ion trap mass spectrometer operated at rough vacuum," Analyst 136, 1305-1309 (2011).

[17] H. Winter and H. W. Ortjohann, "Simple demonstration of storing macroscopic particles in a 'Paul trap'," Am. J. Phys. 59, 807-13 (1991).

[18] Scott Robertson and Richard Younger, "Coulomb crystals of oil droplets," Am. J. Phys. 67, 310-315 (1999).

[19] L. M. Vasilyak, V. I. Vladimirov, L. V. Deputatova, et al., "Coulomb stable structures of charged dust particles in a dynamical trap at atmospheric pressure in air," New J. Phys. 15, 043047 (2013).

[20] http://newtonianlabs.com/.

[21] Earnshaw's theorem is described in some detail at http://en.wikipedia.org/wiki/Earnshaw's_theorem.

[22] M. V. Berry, "The Levitron: An adiabatic trap for spins," Proc. Roy. Soc. A 452, 1207-1220 (1996).

[23] C. Sackett, E. Cornell, C. Monroe, and C. Wieman, "A magnetic suspension system for atoms and bar magnets," Am. J. Phys. 61, 304-309 (1993).

[24] L. D. Landau and E. M. Lifshitz, "Mechanics, 3rd Edition; Course of Theoretical Physics Volume 1," page 93ff, Pergamon Press (1989).

[25] William B. Whitten, Peter T. A. Reilly, and J. Michael Ramsey, “High-pressure ion trap mass spectroscopy,” Rapid Commun. Mass Spectrom. 18, 1749-1752 (2004).

[26] Michael Nasse and Christopher Foot, “Influence of background pressure on the stability region of a Paul trap,” Eur. J. Phys. 22, 563-573 (2001).

[27] Eugene A. Vinitsky, Eric D. Black, and Kenneth G. Libbrecht, “Particle dynamics in damped nonlinear quadrupole ion traps,” arXiv:1409.6262 (2014).

[28] https://www.youtube.com/watch?v=pqfG-df5ZWk (posted 2012), and related images and videos at http://www.paultrap.jecool.net/en/.

[29] B.P. Binks, J.H. Clint, G. Mackenzie, C. Simcock and C.P. Whitby, “Naturally occurring spore particles at planar fluid interfaces and in emulsions", Langmuir 21, 8161-8167 (2005) (Image provided by the authors).

[30] https://www.youtube.com/watch?v=bkYXNeJ8IP0 (posted 2009).